Supporting Information

Fast and ultrafast charge transfer dynamics in organic dye sensitizers anchored on TiO_2 for photoelectrochemical cells

Federica Ruani,[a] Matteo Bartolini,[b] Elena Ermini,[b,c] Elisa Bandini,[a] Andrea Barbieri,[a] Adalgisa Sinicropi,[b,d] Alessandro Mordini,[b,c] Lorenzo Zani*[b] and Barbara Ventura*[a]

[a] Istituto per la Sintesi Organica e la Fotoreattività (ISOF), Consiglio Nazionale delle Ricerche (CNR), Via Gobetti 101, 40129 Bologna BO, Italy.

[b] Istituto di Chimica dei Composti Organometallici (ICCOM), Consiglio Nazionale delle Ricerche (CNR), Via Madonna del Piano 10, 50019 Sesto Fiorentino, Italy.

[c] Dipartimento di Chimica ''U. Schiff'', Università degli Studi di Firenze, Via della Lastruccia 13, 50019 Sesto Fiorentino, Italy.

[d] Dipartimento di Biotecnologie, Chimica e Farmacia, Università di Siena, R^{2}ES Lab, Via Aldo Moro 2, 53100 Siena, Italy.

Corresponding Authors: lorenzo.zani@cnr.it, barbara.ventura@cnr.it

Table of Contents

Synthetic routes of compounds AD418, BTD-DTP1, TTZ5

The dyes used in this study were prepared according to previously reported procedures. The synthetic schemes and a brief description of the synthetic routes are reported below.

AD418 Dye[1]

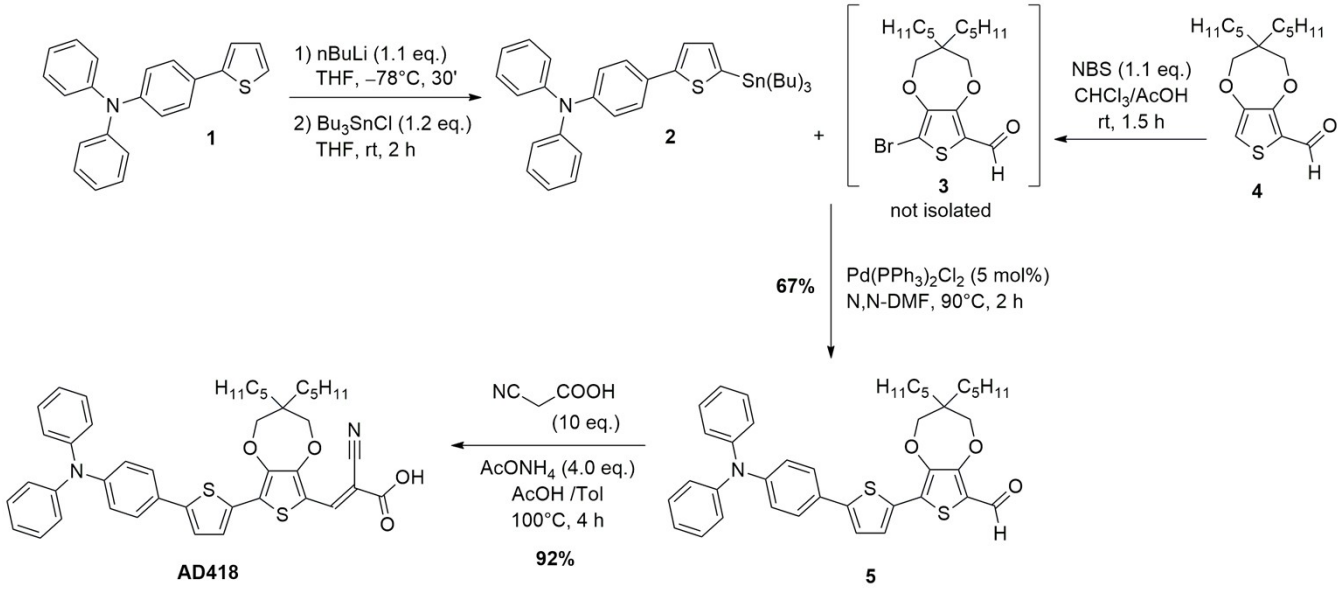

Scheme S1. Optimized synthesis of **AD418** dye.

As shown in Scheme S1, the preparation of compound **AD418** began from the known N,N-diphenyl-4-(2-thienyl)aniline **1**.[2] The remaining C-H bond in 2-position of the thiophene was replaced with a C-Li bond thanks to exposure to *n*-butyllithium, and the metalated intermediate was reacted with tri(*n*-butyl)chlorostannane to yield organostannane **2**. Meanwhile, aldehyde **4** was subjected to electrophilic bromination with *N*-bromosuccinimide to give tetrasubstituted aldehyde **3**, which was not isolated prior to further use to avoid its decomposition. Palladium-catalyzed Stille-Migita cross-coupling between compounds **2** and **3** under typical conditions yielded advanced intermediate **5** in good yield. The latter was finally converted to the desired dye in satisfactory yield by means of a Knoevenagel condensation employing ammonium acetate as the promoter and a mixture of acetic acid and toluene as the solvent. By applying the above synthetic procedure, compound **AD418** could be prepared in >50% yield from starting material **1** in three steps as the longest linear sequence.

BTD-DTP1 dye[3]

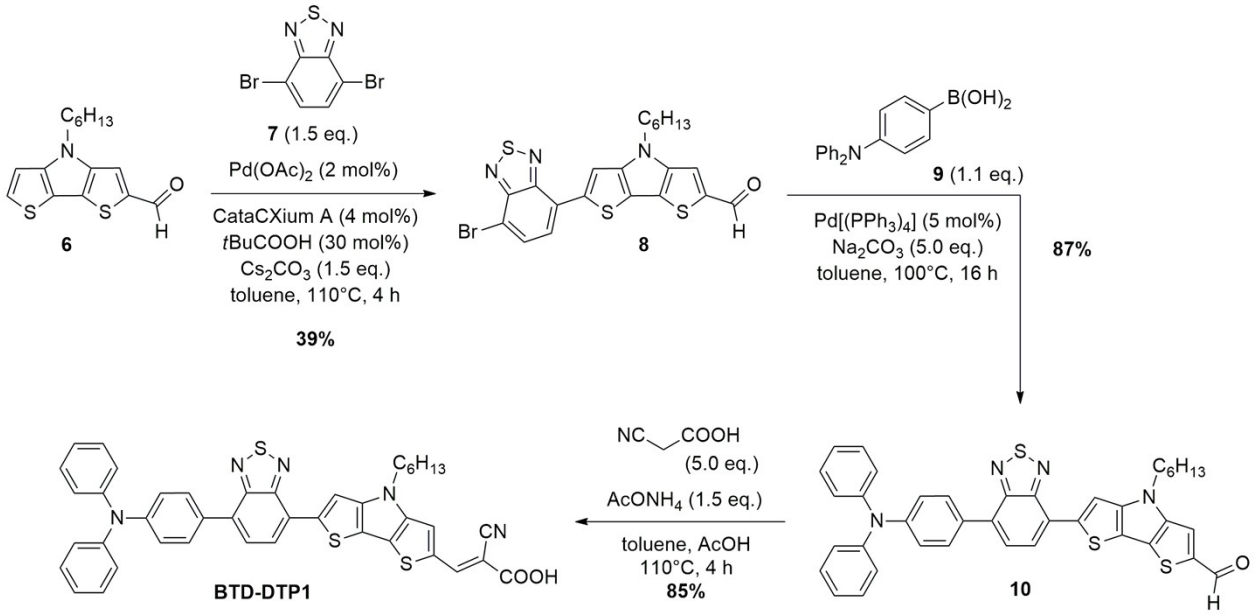

Scheme S2. Optimized synthesis of **BTD-DTP1** dye.

The synthesis of compound **BTD-DTP1** (Scheme S2) started from aldehyde **6**, previously obtained according to a known procedure.[4] This compound was reacted with 4,7-dibromo-2,1,3-benzothiadiazole (**7**) by means of a direct arylation procedure catalyzed by a palladium complex formed in situ from $Pd(OAc)_2$ and ligand *bis*(adamantyl)-*n*-butylphosphine (CataCXium A®), providing product **8** in moderate yield. The latter was then subjected to a Pd-catalyzed Suzuki-Miyaura cross-coupling with boronic acid **9** under typical conditions, which proceeded in good yield and allowed to install the donor group of the final compound, reaching advanced intermediate **10**. Finally, the latter underwent Knoevenagel condensation with cyanoacetic acid under conditions similar to those seen above for the synthesis of **AD418**, furnishing the desired compound in 85% yield. By applying the above synthetic procedure, compound **BTD-DTP1** could be prepared in 29% yield from compound **6** in three linear steps.

TTZ5 Dye[5]

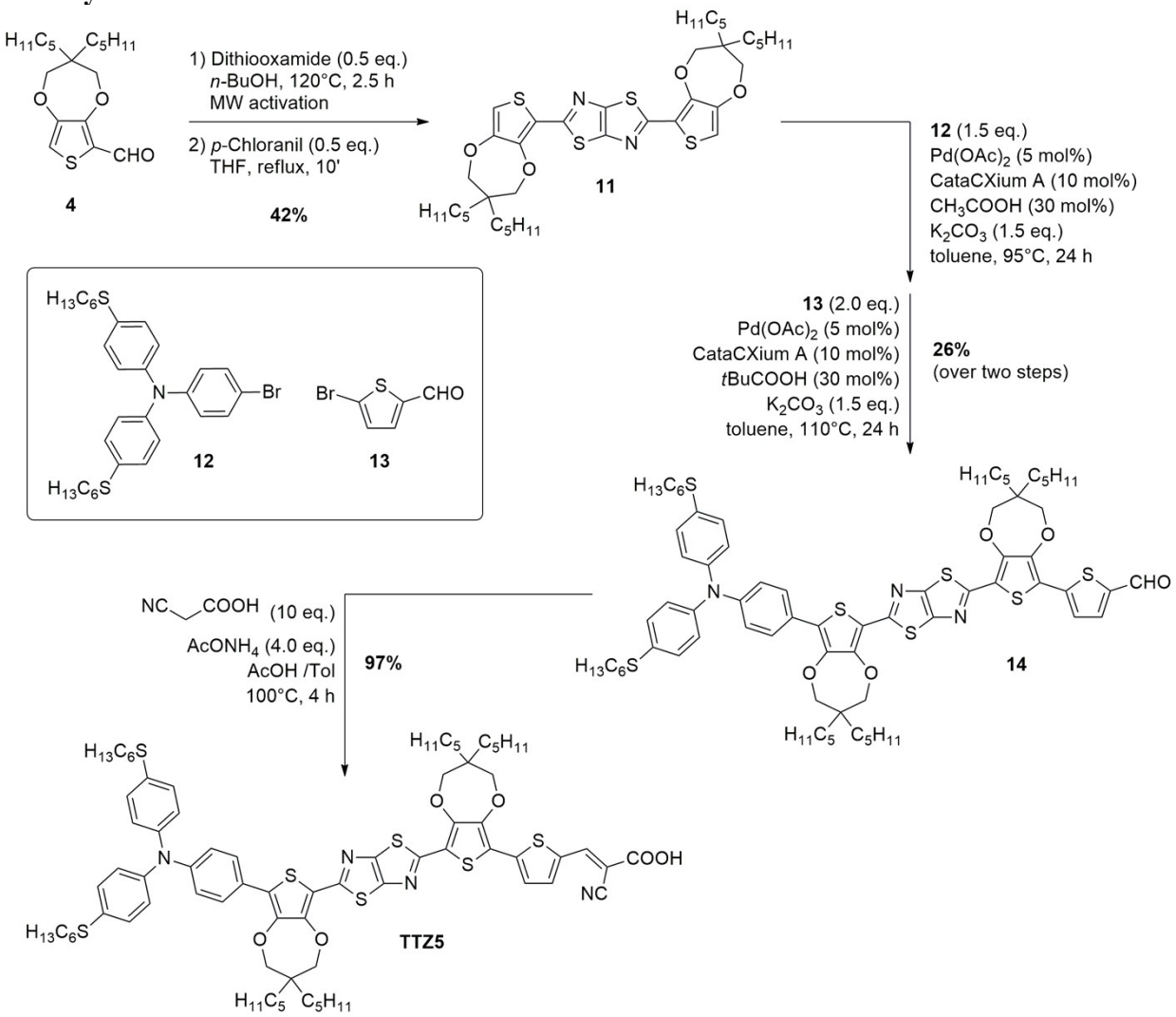

Scheme S3. Optimized synthesis of **TTZ5** dye.

As shown in Scheme S3 the synthesis of sensitizer **TTZ5** can be divided in three parts:

a) A microwave-activated one-pot condensation/oxidation sequence of the aldehyde **4** (seen above for the synthesis of **AD418**) with dithiooxamide to achieve the preparation of thiazolothiazole (TzTz) **11** in moderate yield.

b) A one-pot, telescopic Pd-catalyzed direct arylation reaction to sequentially introduce into the TzTz scaffold the donor (**12**) and the acceptor (**13**) groups. Despite the moderate yield, the application of precisely optimized reaction conditions allowed to replace the previous Suzuki-Miyaura-based route,[6] bringing significant improvements in terms of the number of synthetic and purification steps, waste production and overall cost.

c) A Knoevenagel condensation with cyanoacetic acid under condition analogous to those seen above, to attach the anchoring group and obtain the final **TTZ5** dye with excellent yield.

According to the above procedure, dye **TTZ5** was prepared with a yield of approx. 12% along 4 linear steps from aldehyde **4**. A more detailed description of the synthetic procedure as well as experimental details can be found in the original publication.

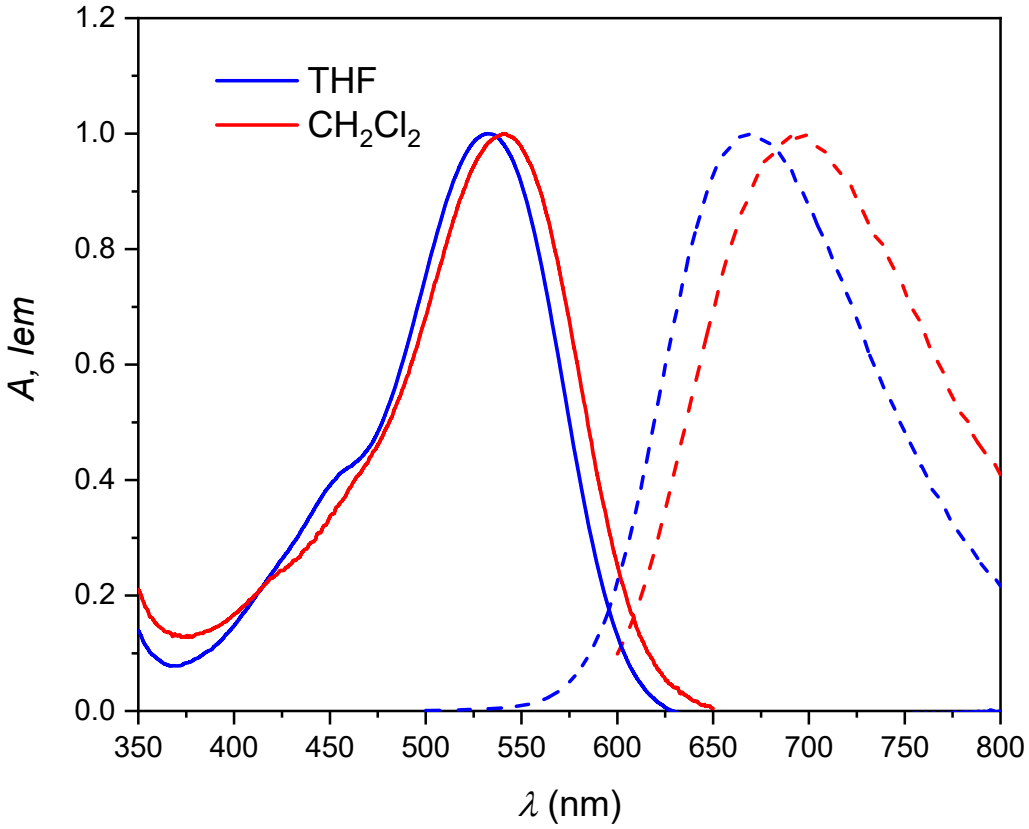

Figure S1. Normalized absorption (full line) and corrected emission (dotted line, λ_{exc} = 530 nm) spectra of **BTD-DTP1** in THF (blue) and CH_2Cl_2 (red) solutions at room temperature.

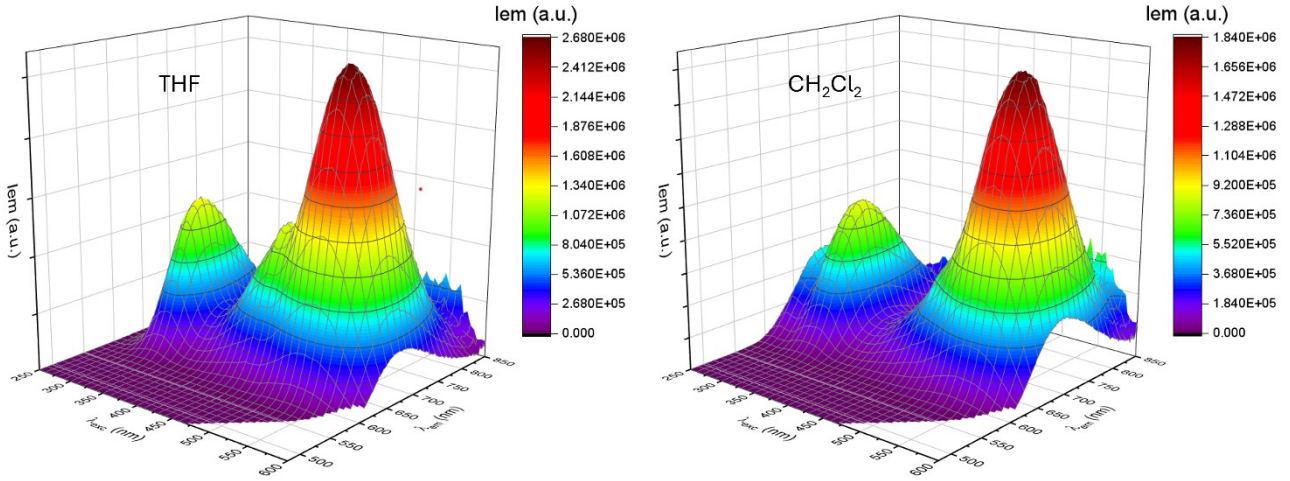

Figure S2. Corrected 3D emission maps of **BTD-DTP1** in THF (a) and CH_2Cl_2 (b) solutions at room temperature.

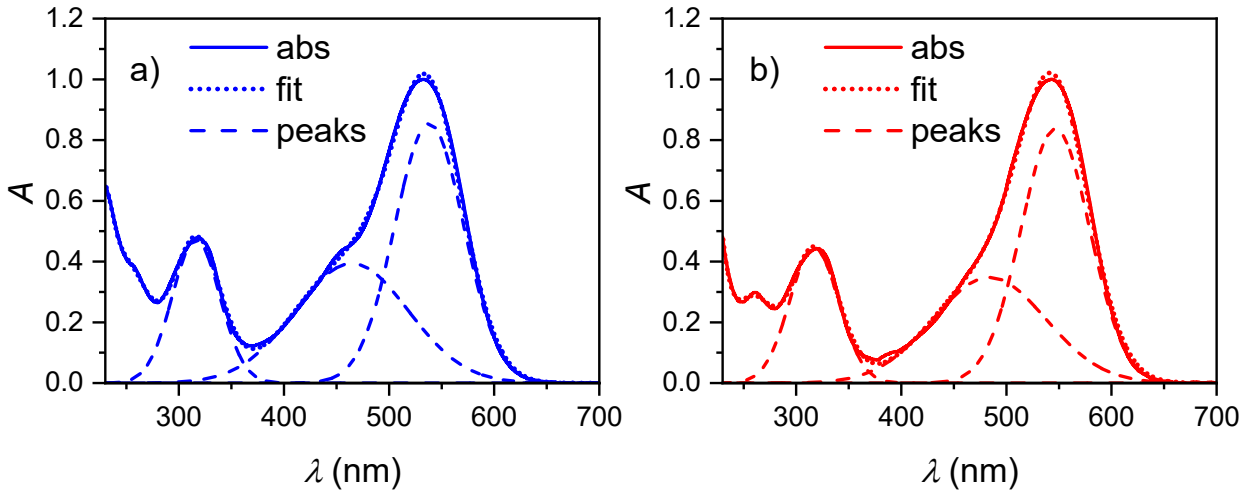

Figure S3. Normalized absorptions (full line), fittings obtained from multi-peak fitting with gaussian functions (dotted) and the three main deconvoluted peaks (dashed) for **BTD-DTP1** sample in THF (a) and CH_2Cl_2 (b).

Table S1. CAM-B3LYP/6-311G(d,p) computed absorption maxima (λ^{a}_{max}), excitation energy (E_{exc}), and oscillator strengths (f) for the first ten singlet excited states of **BTD-DTP1** in THF.

Excited state	**λ^{a}_{max} (nm)**	**E_{exc} (eV)**	**f_{exc}**	**Transition (%, > 10%)**
1	515	2.41	1.98	74 (H→L) 15 (H-1→L)
2	408	3.04	0.24	30 (H-1→L) 49 (H→L+1)
3	374	3.31	0.07	83 (H-2→L) 12 (H-2→L+1)
4	364	3.41	0.08	40 (H-1→L) 28 (H-1→L+1) 14 (H→L+1)
5	305	4.07	0.01	20 (H-3→L) 19 (H-2→L+1) 16 (H-1→L+1) 17 (H→L+1)
6	302	4.10	0.06	47 (H-2→L+1) 10 (H-1→L+1)
7	298	4.16	0.27	21 (H-3→L) 39 (H→L+2)
8	290	4.27	0.03	22 (H-1→L+3) 55 (H→L+3)
9	288	4.31	0.26	27 (H-3→L) 14 (H-1→L+1) 12 (H→L+2)
10	283	4.38	0.15	14 (H-9→L) 25 (H-8→L) 12 (H-8→L+1)

Table S2. B3LYP/6-31G* electron density distributions and energies (eV) of the HOMOs and LUMOs orbitals of **BTD-DTP1** in THF.

H-9	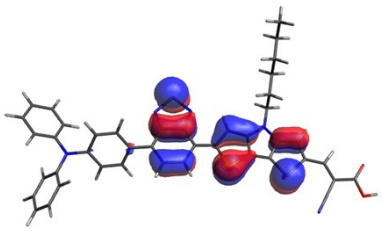	-7,327
H-8	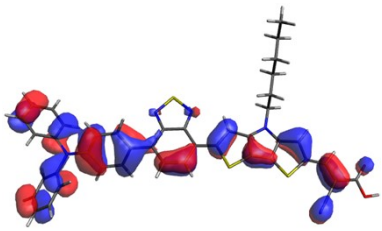	-7,233
H-3	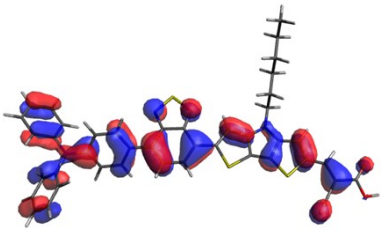	-6,482
H-2	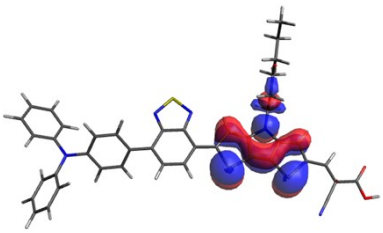	-6,026
H-1	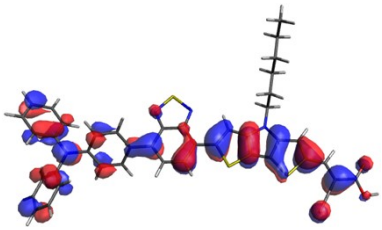	-5,492
H	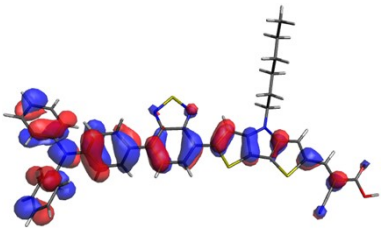	-5,013

L	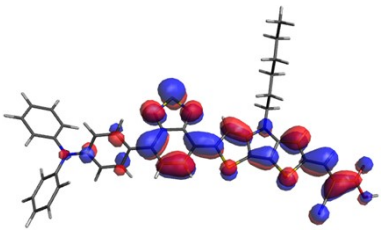	-2,866
L+1	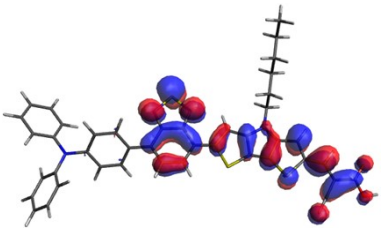	-2,339
L+2	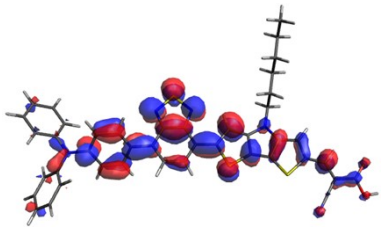	-1,062
L+3	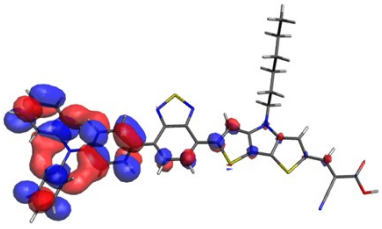	-0,514

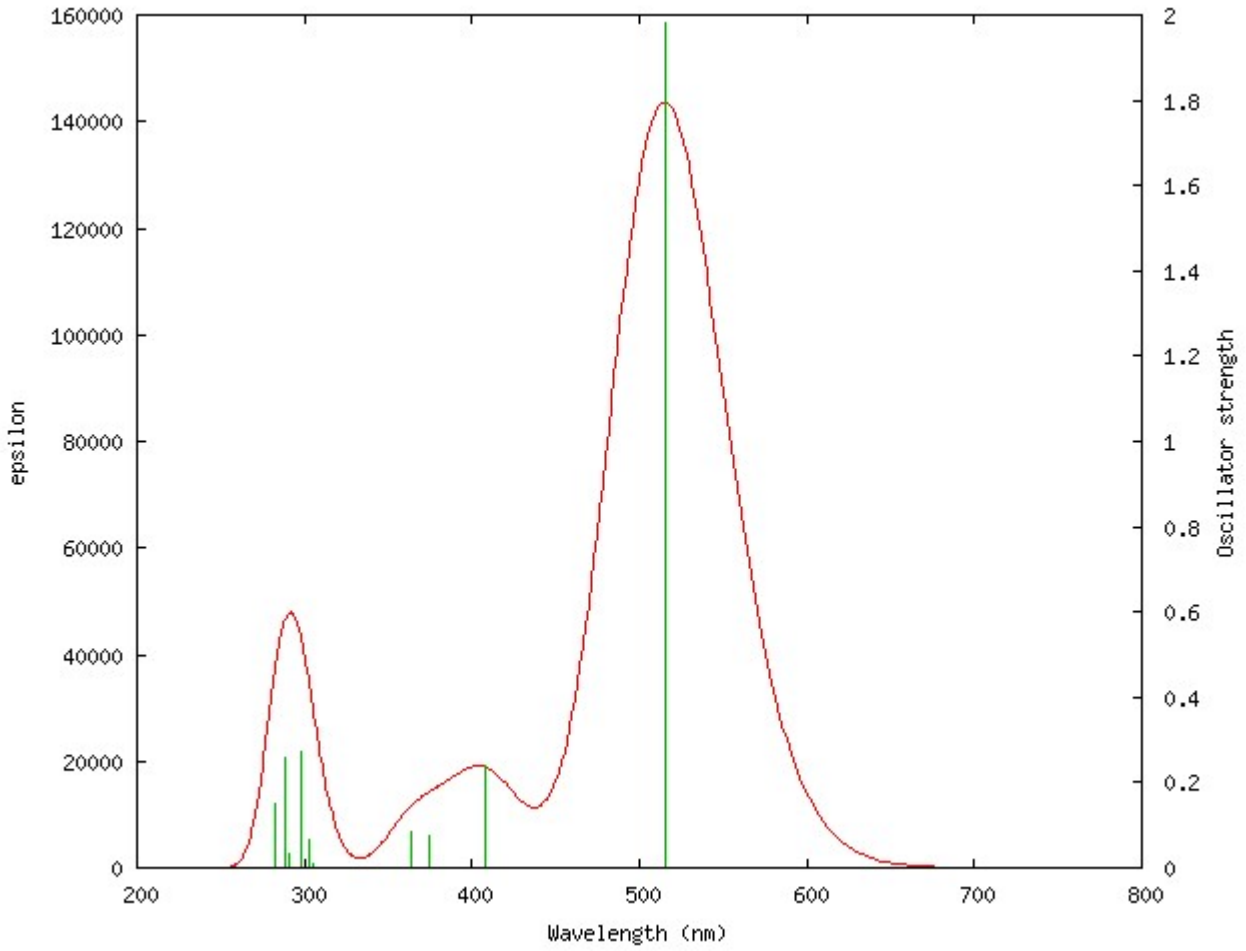

Figure S4. UV–Vis spectrum of **BTD-DTP1** simulated with GaussSum-2.2.6.1 considering a gaussian broadening (FWHM = 3000 cm-1) of the calculated transition energies.

Table S3. Emission decay parameters of **BTD-DTP1** in THF and CH_2Cl_2 solutions at rt.

	τ_1 (ns)	% τ_1	τ_2 (ns)	% τ_2
THF	2.6	80	4.7	20
CH_2Cl_2	2.0	94	5.6	6

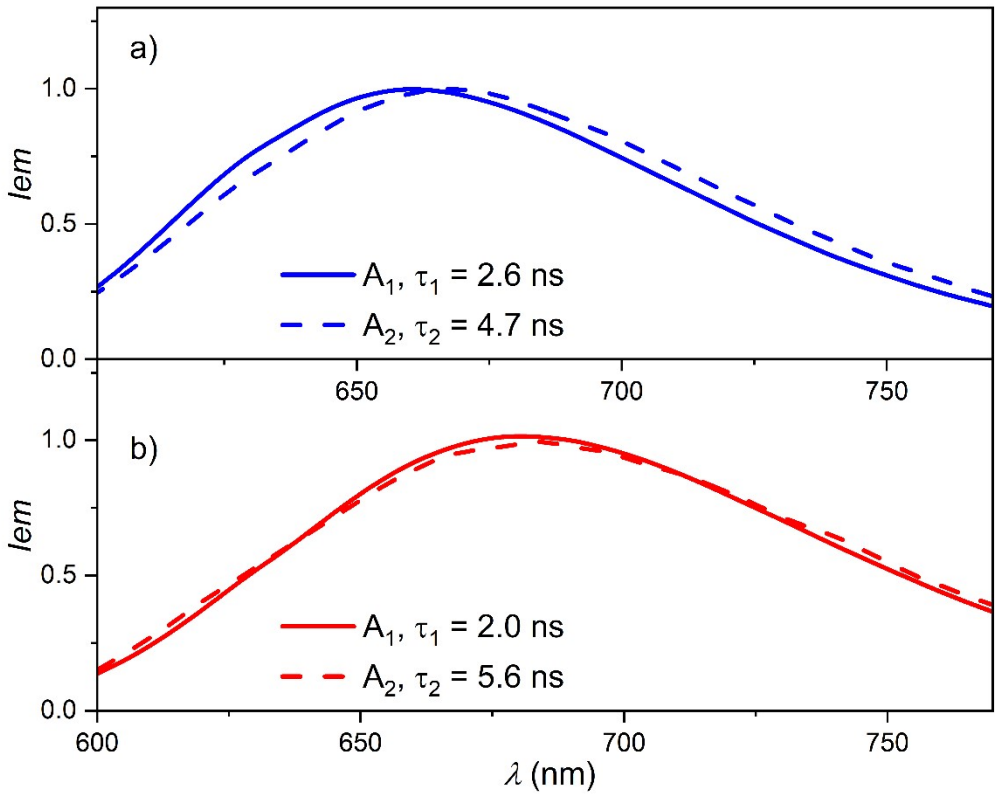

Figure S5. Normalized spectral distributions of pre-exponential amplitudes of calculated lifetimes from global fit analysis performed with TCSPC (λ_{exc} = 510 nm) of **BTD-DTP1** in THF (a) and CH_2Cl_2 (b) solutions. The spectra are corrected for the detector wavelength's dependent response.

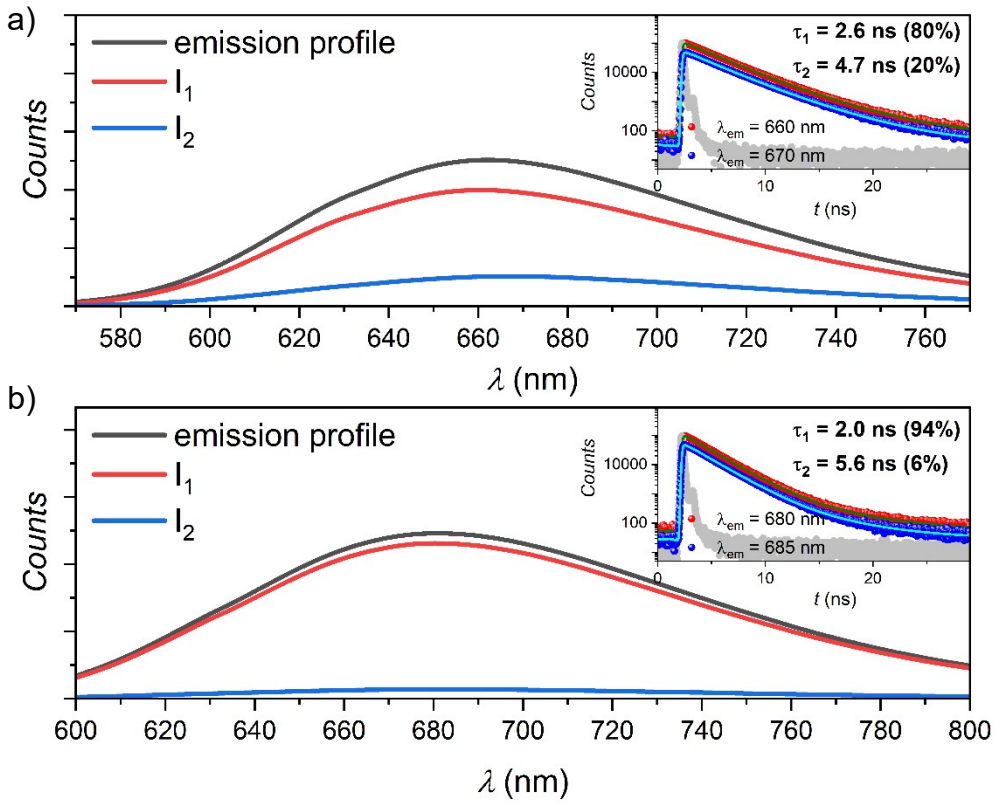

Figure S6. Decay associated spectra of **BTD-DTP1** in THF (a) and CH_2Cl_2 (b) solutions from global fit analysis performed with TCSPC (λ_{exc} = 510 nm). The steady-state emission spectrum is also reported for comparison (black line). The spectra are corrected for the detector wavelength's dependent response. In the inset, the decays collected at the maximum emission wavelength for each spectral profile are reported, together with the relative fittings.

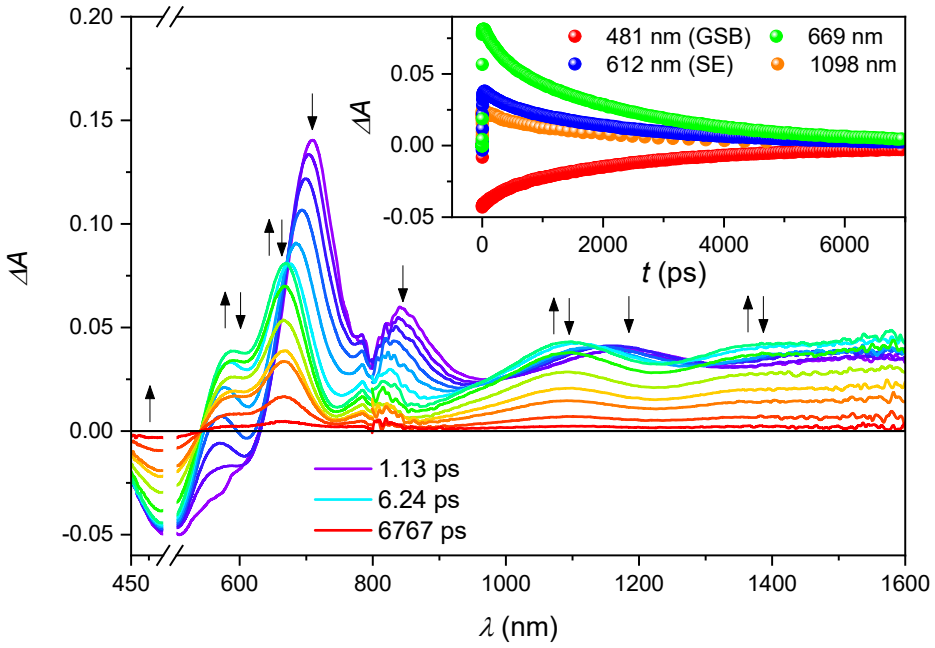

Figure S7. TA spectral evolution of **AD418** in THF (λ_{exc} = 500 nm, E = 3 μJ/pulse). Inset: TA kinetics at selected wavelengths with the relative fittings (lines).

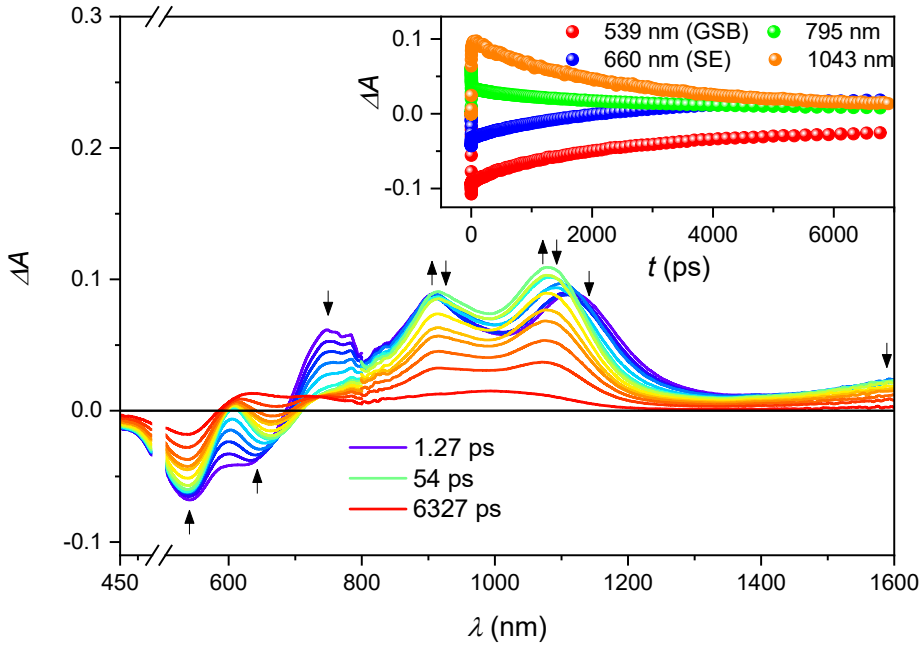

Figure S8. TA spectral evolution of **BTD-DTP1** in THF (λ_{exc} = 500 nm, E = 3 μJ/pulse). Inset: TA kinetics at selected wavelengths with the relative fittings (lines).

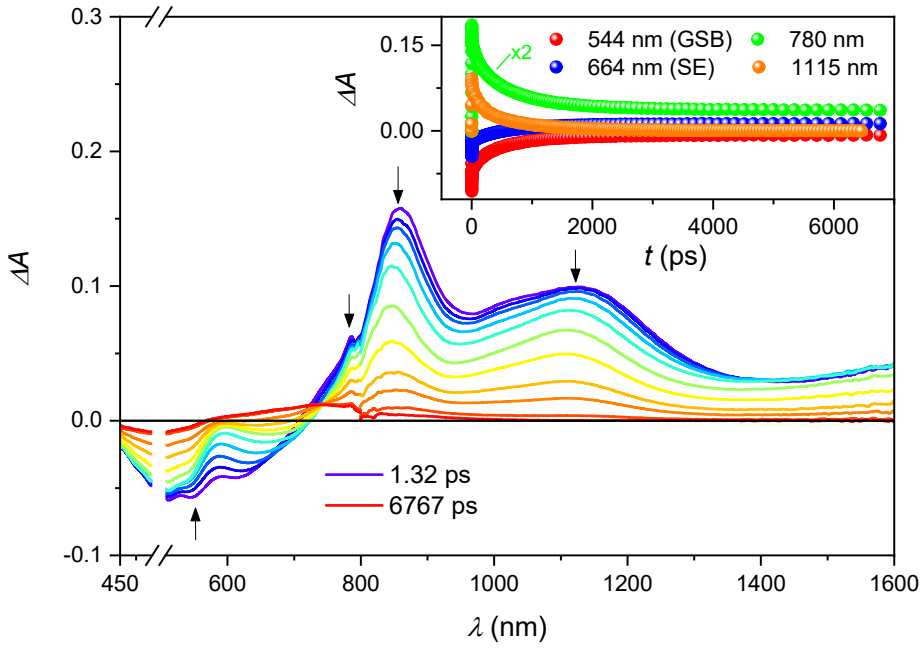

Figure S9. TA spectral evolution of **TTZ5** in THF (λ_{exc} = 500 nm, E = 3 μJ/pulse). Inset: TA kinetics at selected wavelengths with the relative fittings (lines).

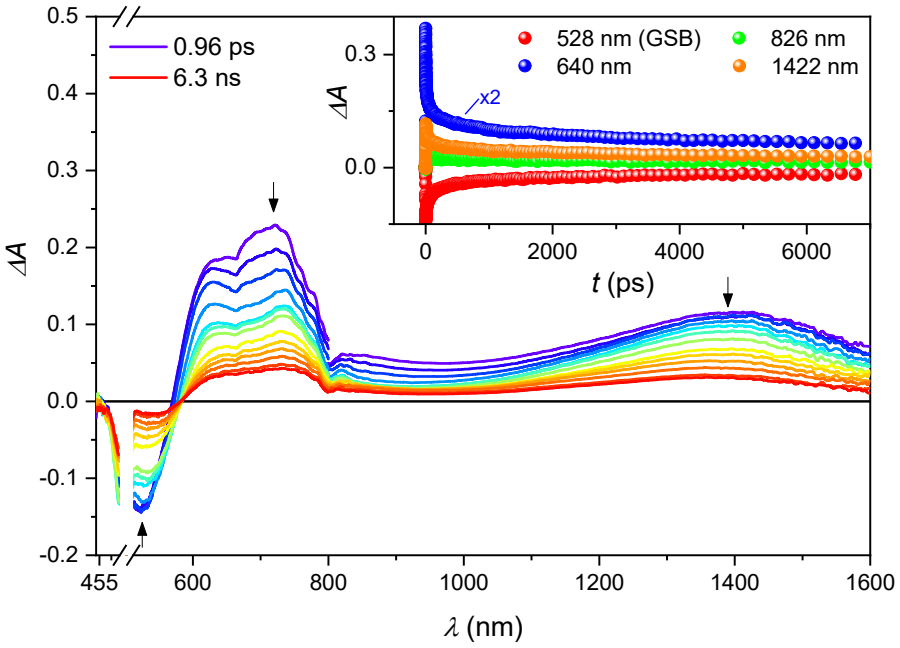

Figure S10. TA spectral evolution of **AD418** on TiO_2 (λ_{exc} = 500 nm, E = 3 μJ/pulse). Inset: TA kinetics at selected wavelengths with the relative fittings (lines).

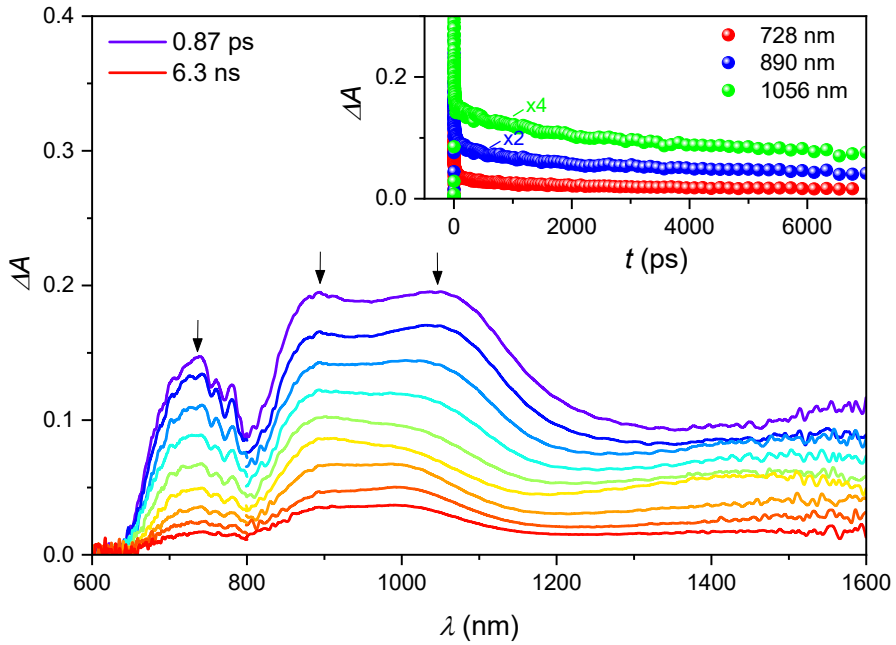

Figure S11. TA spectral evolution of **BTD-DTP1** on TiO_2 (λ_{exc} = 500 nm, E = 3 μJ/pulse). Inset: TA kinetics at selected wavelengths with the relative fittings (lines).

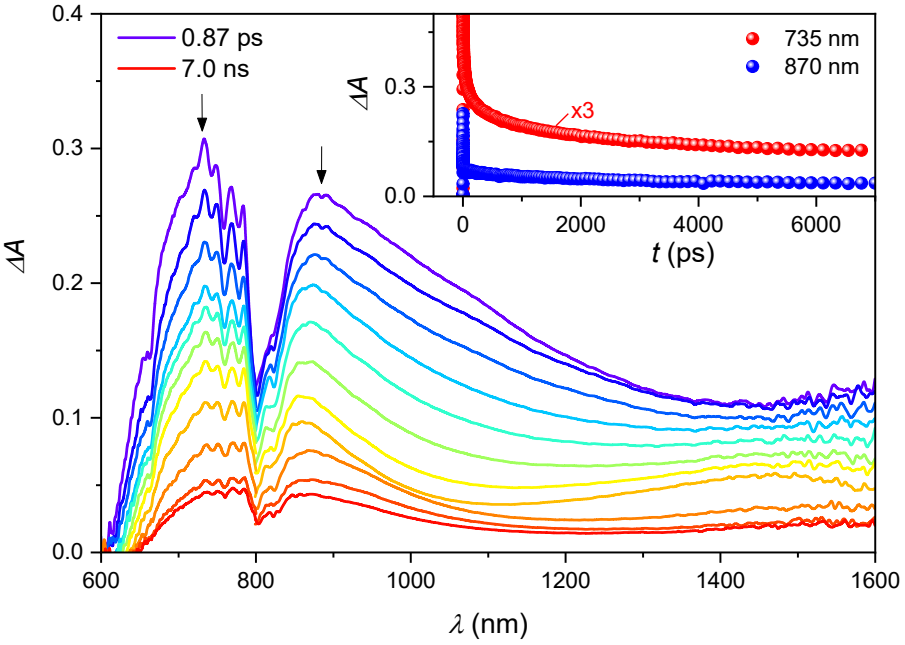

Figure S12. TA spectral evolution of **TTZ5** on TiO_2 (λ_{exc} = 500 nm, E = 3 μJ/pulse). Inset: TA kinetics at selected wavelengths with the relative fittings (lines).

References

1. A. Dessi, M. Monai, M. Bessi, T. Montini, M. Calamante, A. Mordini, G. Reginato, C. Trono, P. Fornasiero and L. Zani, *ChemSusChem*, 2018, **11**, 793-805.
2. W. Li, C. Du, F. Li, Y. Zhou, M. Fahlman, Z. Bo and F. Zhang, *Chem. Mater.*, 2009, **21**, 5327-5334.
3. A. Dessì, D. A. Chalkias, S. Bilancia, A. Sinicropi, M. Calamante, A. Mordini, A. Karavioti, E. Stathatos, L. Zani and G. Reginato, *Sustain. Energy Fuels*, 2021, **5**, 1171-1183.
4. P. Y. Ho, Y. Wang, S. C. Yiu, W. H. Yu, C. L. Ho and S. Huang, *Org. Lett.*, 2017, **19**, 1048-1051.
5. M. L. Parisi, A. Dessi, L. Zani, S. Maranghi, S. Mohammadpourasl, M. Calamante, A. Mordini, R. Basosi, G. Reginato and A. Sinicropi, *Front. Chem.*, 2020, **8**, 214.
6. A. Dessì, M. Calamante, A. Mordini, M. Peruzzini, A. Sinicropi, R. Basosi, F. Fabrizi de Biani, M. Taddei, D. Colonna, A. di Carlo, G. Reginato and L. Zani, *RSC Adv.*, 2015, **5**, 32657-32668.